

Offline Pulse-Shape Discrimination Algorithms for Neutron Spectrum Unfolding

Marek Flaska and Sara A. Pozzi, *Members, IEEE*

Abstract—An optimized fast pulse-shape discrimination algorithm is used to discriminate neutrons from gamma rays with high accuracy, in a mixed radiation field. The discriminated data is subsequently used to identify the source. Experimental pulse-height distributions from discriminated data are shown for Cf-252 and Am-Be sources and are compared with simulations performed with the MCNP-PoliMi code. In all cases, very good agreement between simulations and measurements was achieved. In addition, several source-shielding configurations are presented to assess the influence of the potential source shielding on the measured neutron pulse-height distribution.

I. INTRODUCTION

ACCURATE knowledge of neutron energy spectra is of great interest in many areas, such as nuclear nonproliferation, international safeguards, nuclear material control and accountability, national security, and counterterrorism. In particular, for safeguards applications, a fast and robust method for the identification of typical neutron sources (Cf-252, Am-Be, etc.) is essential. The identification of the neutron sources by unfolding the initial neutron energy spectrum is a very promising method, based on the observable differences in the spectra of the different sources.

Neutron and gamma-ray pulse-shape discrimination (PSD) is a well-known technique used in mixed neutron/gamma-ray radiation fields and is frequently used with organic liquid scintillation detectors [1-3]. The liquid scintillators, which are sensitive to both neutron and gamma-ray radiation, are often used in nonproliferation applications due to their excellent neutron/gamma-ray PSD properties. The decision time of the PSD techniques is required to be very short in order to perform measurements at high count rates. This allows for a high sensitivity of the assays performed on nuclear materials with the main objective to detect and to determine the mass and composition of these materials [4].

After the neutron and gamma-ray pulses were measured with the liquid scintillator and the neutron distribution was obtained from the discriminated data, a certain neutron unfolding technique can be applied [5]. However, since even a small variation in the measured distribution leads to a large variation in the unfolded neutron spectrum, it is crucial to identify neutrons with very high accuracy. This requires the

high degree of accuracy in the separation of the neutrons from the gamma rays typically present in the background. In this paper, we present the results of the analysis of a large number of neutron and gamma-ray pulses with a liquid scintillator BC-501A using a Tektronix digital oscilloscope TDS-5104. A PSD technique based on pulse integration over different time periods was optimized and applied to discriminate neutrons from gamma rays. Two neutron sources were used for investigation: a Cf-252 and an Am-Be source. In addition, measured pulse-height distributions were compared with those simulated by using the MCNP-PoliMi code [6]. Finally, several source-shielding configurations were tested to assess the influence of the potential source surrounding on the measured pulse-height distribution.

II. STRUCTURE OF THE INVESTIGATION

The main structure of the investigation is shown in Fig. 1. In this paper, we describe the first three steps in detail. The last steps are being performed, and will be presented in a future publication.

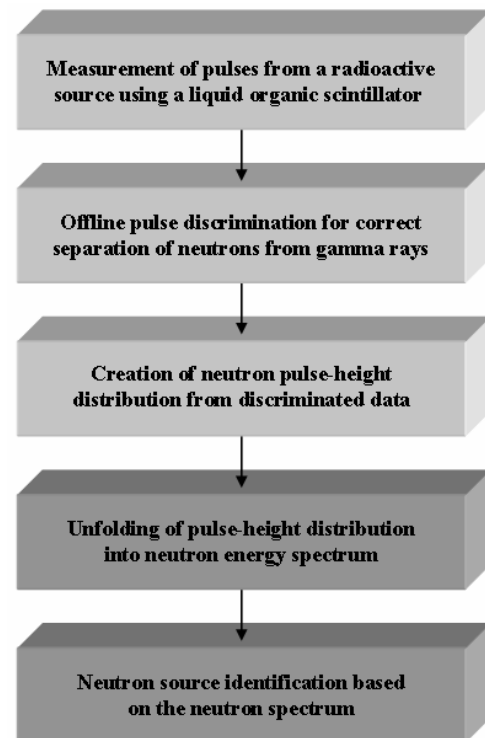


Fig. 1. The flowchart of the investigation. The first three steps are described in this paper.

Manuscript received November 17, 2006. This work was supported by the Oak Ridge National Laboratory and U.S. Department of Energy, National Nuclear Security Administration, Office of Nonproliferation Research Engineering (NA-22).

M. Flaska is with the Oak Ridge National Laboratory, Oak Ridge, TN 37831 USA (telephone: 865-574-5486, e-mail: flaskam@ornl.gov).

S. A. Pozzi is with the Oak Ridge National Laboratory, Oak Ridge, TN 37831 USA (telephone: 865-574-5699, e-mail: pozzisa@ornl.gov).

III. DATA ACQUISITION

A fast waveform digitizer, digital oscilloscope Tektronix TDS-5104 with a 1-GHz resolution, was used to store tens of thousands of pulses from the liquid scintillator BC-501A for subsequent analysis. The oscilloscope fast-frame acquisition mode allowed for capturing the pulses with a resolution of 0.2–0.4 ns. The detector BC-501A is built of a cylindrical liquid organic scintillator model 4.62MAB-1F3BC-501A/5, which is 7.7 cm thick with a diameter of 15.2 cm. The detector container is made of aluminum. The front face of the detector has a thickness of 2 mm. The side wall is composed of two layers: the external layer has a thickness of 2 mm and the internal layer is approximately 0.5 mm thick. The photomultiplier tube is mounted on the back circular surface of the detector.

To optimize the PSD method by using particle-attributed pulses, neutrons and gamma rays were measured from two known radioactive sources. The neutrons emitted by a Cf-252 source were detected using the time-of-flight (TOF) method to identify the neutrons in a gamma-ray background. Exceptions for misidentification of neutrons are accidental coincidences, which result in gamma-ray pulses being attributed as neutron pulses. The Cf-252 source was placed in an ionization chamber at a distance of 1 m from the detector. The ionization chamber served as a “start” detector to determine the time zero. The neutron pulses obtained with this method have been named “TOF attributed neutrons.”

The gamma-ray pulses were measured using a Cs-137 source placed on the face of the detector. These gamma-ray pulses are named “gamma rays” in the remainder of this paper.

IV. OPTIMIZATION OF THE PSD METHOD

It is well known that the total light output generated in the scintillator can be represented by the sum of two exponential decays referred to as the fast and slow components of the scintillation process. The fraction of the total light observed in the slow component is a function of the type of particle inducing the scintillation. In general, the slow component is larger for heavier particles (i.e., the tails of the average neutron pulses are consistently greater than the tails of the gamma-ray pulses) [7]. This difference in the intensity of slow neutron and gamma-ray components serves as a basis for the PSD method.

The applied offline PSD technique is based on the charge integration method, in which integrals over different time periods are compared to specify the type of the particle producing the pulse in the detector. However, in this case, the method is applied to digitized pulses with height values in units of voltage (V); thus integration over any time period results in values in units of V*ns.

Following the discussion above, a ratio of two areas is used for the particle identification. The ratio is obtained by integration of the pulse over different time intervals. The first area is the total area of the pulse (A_1); the second area is the

tail of the pulse (A_2). These areas are shown schematically in Fig. 2.

The area ratio is defined as

$$R = \frac{A_2}{A_1} \quad (1)$$

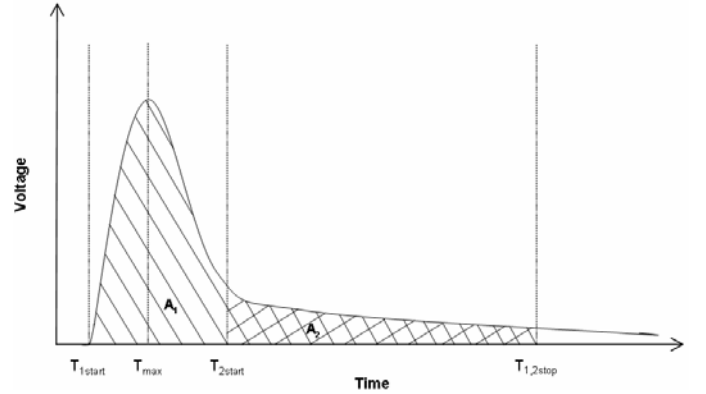


Fig. 2. Visualization of the areas used to calculate the ratio for the discrimination of neutrons from gamma rays.

The tail integral A_2 is calculated from a certain point above the pulse maximum (see T_{2start} in Fig. 2) to the end of the pulse ($T_{1,2stop}$). In the case presented in Fig. 3, $T_{2start} = T_{max} + 6ns$, while $T_{1,2stop} - T_{max} = 110ns$. The latter is given by the time range used in our measurements and is valid for all results discussed later in this paper. In contrast, the total integral A_1 is calculated by integrating between the values T_{1start} and $T_{1,2stop}$; thus it covers the entire pulse area.

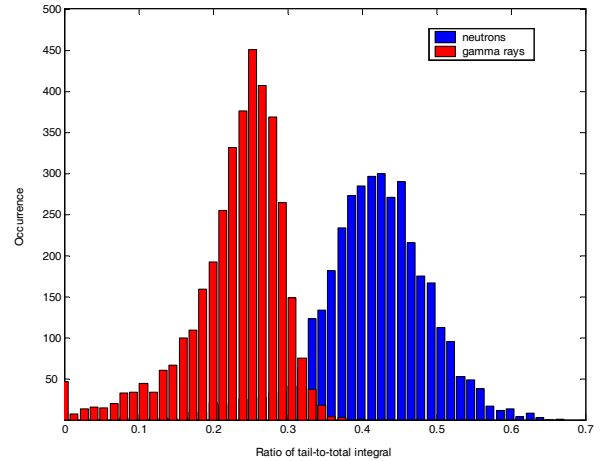


Fig. 3. Typical histograms for neutron and gamma-ray pulses. Two distributions can be clearly distinguished.

The integral ratio R is clearly larger for most of the neutron pulses when compared to the gamma-ray pulses. The relatively high value occurring in the gamma-ray histogram at position zero is due to the accumulation of low ratio values (negative values are not possible). Fig. 4 shows the distributions created from the histogram in Fig. 3. The cross point of the neutron and the gamma-ray curve has been chosen

as a discrimination point to classify the particles detected. The point in this particular case lies at a value of $R=0.32$. This value has not been optimized. Above the classification point, all pulses are classified as neutrons, while below this point, the pulses are classified as gamma rays. It can be seen in Fig. 4 that a certain number of neutrons and gamma rays are “misclassified” when using this technique. Therefore, optimization of this method is required.

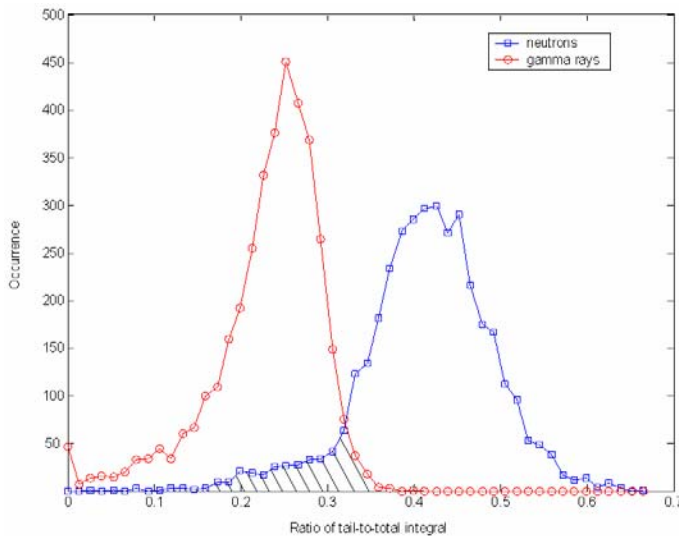


Fig. 4. Curves created from the neutron and gamma-ray histograms shown in Fig. 3. The “overlap area” is marked.

The number of misclassified neutrons and gamma rays was minimized by optimizing the integration range of the tail integral and the location of the classification point. In fact, an increase of the integration range of the total integral would also lead to additional minimization of the overlap area. This is because the slow component of the light produced by the liquid scintillator BC-501A reaches beyond 300 ns [8]. However, in the TOF measurements, the pulse range was limited to 130 ns, thus this value could not be increased.

Fig. 5 shows the overlap area as a function of the starting point of the tail integral A_2 . The upper limit for the tail integral was fixed to 110 ns. The x-axis in Fig. 5 is the time shift from the pulse maximum toward positive values (i.e., $T_{2start} - T_{max}$). As shown in Fig. 5, the overlap area reaches its minimum around 11 ns. At this point, the total overlap area reaches the minimum value of 3% from the total area of the neutron and gamma-ray distributions. For this reason, this value has been chosen as optimal for the tail integration. When using this value, the tail integral A_2 has a total range of 99 ns. The pulse-height threshold was set to 0.07 MeVee.

Fig. 6 shows the neutron and gamma-ray histograms obtained using the optimized tail integral. In Fig. 6 there is even higher occurrence in the gamma-ray histogram at position zero than that shown in Fig. 3. This is due to additional accumulation of low ratio values. This accumulation takes place as a result of shifting the neutron and gamma-ray histograms to lower values by shifting the starting point of the tail integral toward positive values. It is

apparent that in this case the optimal classification point lies below 0.32, which is the value deduced from Fig. 4.

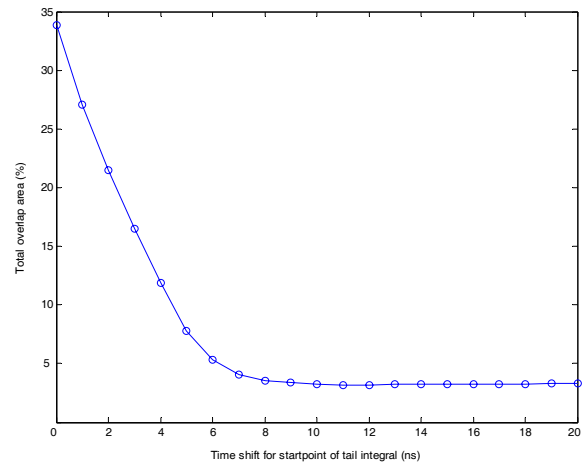


Fig. 5. Total overlap area as a function of the starting point of the tail integral. The x-axis is given by $T_{2start} - T_{max}$.

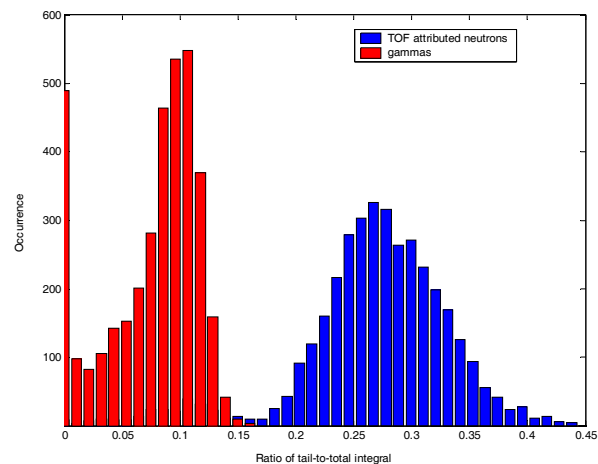


Fig. 6. Histograms of neutron and gamma-ray pulses obtained by using the optimized range of the tail integral.

Fig. 7 shows the number of misclassified neutrons and gamma rays as a function of the location of the classification point. As mentioned previously, all pulses (both neutron and gamma ray) are classified as neutrons when lying above this point, while those below this point are classified as gamma rays. Fig. 7 shows that this condition is, in this particular case, fulfilled by choosing the classification point at a value of 0.15. At this point, approximately 3% of pulses are misclassified. Most of these pulses are neutrons, which means that almost no gamma rays are misclassified using the known pulses. The units of the x-axis in Fig. 7 are identical to those shown in Fig. 6.

Fig. 8 shows the tail integral A_2 as a function of the total integral A_1 . Apparently, some TOF attributed neutron pulses are located in the gamma-ray area. In fact, these pulses are gamma rays that were accidentally identified as neutrons.

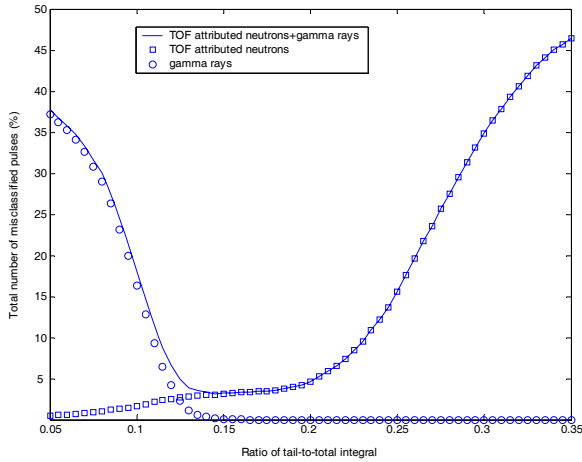


Fig. 7. Total overlap area as a function of the ratio of the tail-to-total integral. The ratio of 0.15 was chosen as the optimal value.

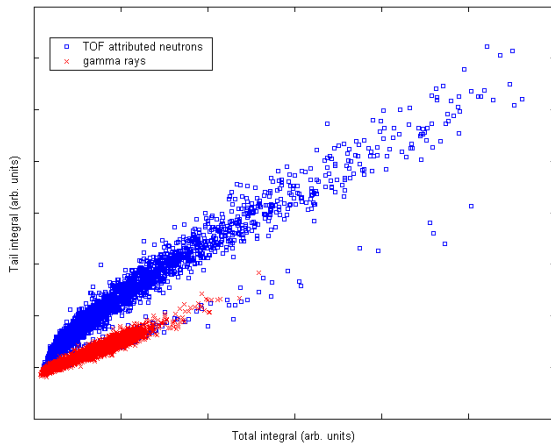


Fig. 8. The tail integral versus the total integral. TOF-attributed neutron and known gamma-ray pulses are well separated. Some pulses attributed to neutrons lie in the gamma-ray area.

V. APPLICATION OF THE OPTIMIZED PSD METHOD TO UNKNOWN PULSES

The digital oscilloscope, scintillation detector, and Cf-252 neutron source described in Section III were used. In addition, an Am-Be source was tested, and several shielding bars were used. In particular, 1-in. lead (Pb) and 1-in. polyethylene (PE) blocks were positioned between the source and the detector, while the source-detector distance was fixed to 50 cm. In the measurement no TOF method was applied, so neutrons were discriminated from the gamma rays by using the PSD technique discussed earlier. The data were collected at a rate of 5 GS/s. Several cases were investigated using both sources and different shielding conditions. The shielding between the source and the detector served to simulate a possible presence of material during in-the-field investigations. An example of the experimental setup is shown in Fig. 9, in which the Am-Be source and the BC-501A are shown, together with the Pb block. In all cases, the pulse-height threshold was set to 0.094 MeVee.

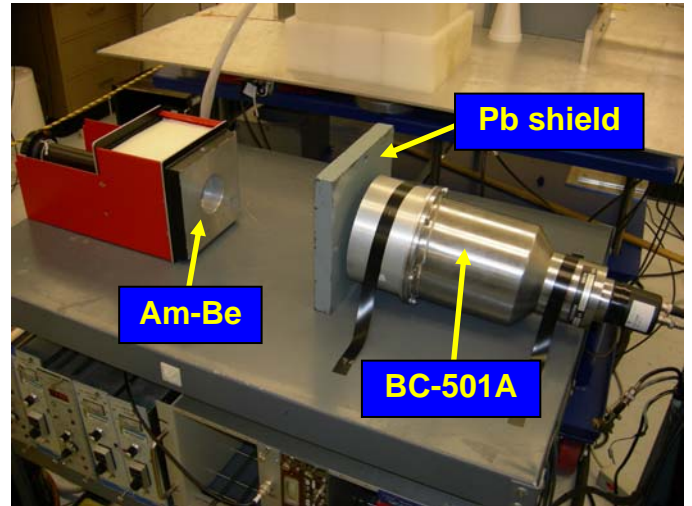


Fig. 9. An example of the measurement setup used to test the optimized pulse-shape discrimination method.

The MCNP-PoliMi code was used to simulate the pulse-height distributions for different source-detector configurations. This code allows for accurate simulations resulting from correctly modified secondary particle production in the MCNP-PoliMi. Another advantage of the MCNP-PoliMi code is that detailed information on the interactions of neutrons and gamma rays inside user-defined cells (typically detectors) are printed to a collision output file. These collisions are then analyzed with a dedicated postprocessing code, which takes into account all important properties of the detector [9].

Fig. 10 shows the histogram for the configuration Cf-252 with the 1-in. Pb block. The neutron distribution is very well separated from the gamma-ray distribution, which allows for accurate discrimination of the neutrons from the gamma-rays.

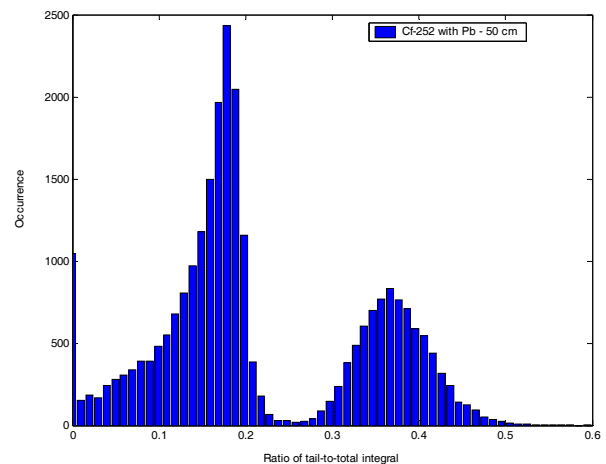


Fig. 10. Histogram for the configuration Cf-252 – 1-in. Pb block. The source-detector distance was 50 cm.

The shield allowed the relative number of neutron pulses acquired to increase due to elimination of some source gamma rays, compared to the bare case.

Figs. 11 and 12 show the pulse-height distributions from the Cf-252 with no shield and 1-in. Pb shield, respectively. The x-axis is given in MeVee, and represents the light output from the detector. The discriminated neutron data are compared with the MCNP-PoliMi simulations. A very good agreement has been achieved. In Fig. 12, it can be seen that the presence of the Pb block improves the quality of the measured data by increasing the number of neutron pulses per data acquisition (the total number of pulses per acquisition was constant).

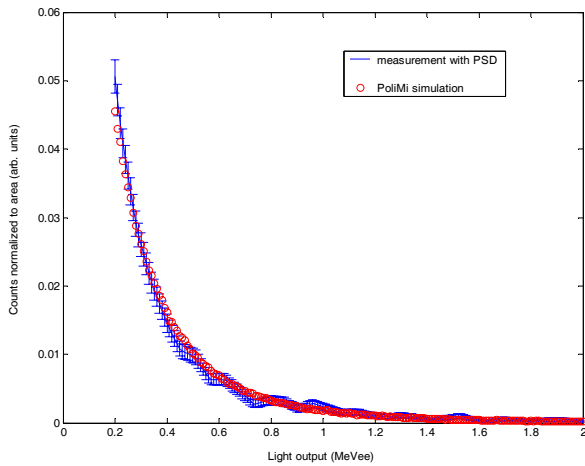


Fig. 11. Measurement versus simulation for the case Cf-252 – no shield. The optimized PSD method was applied to the measured data. The simulation was performed with the MCNP-PoliMi code.

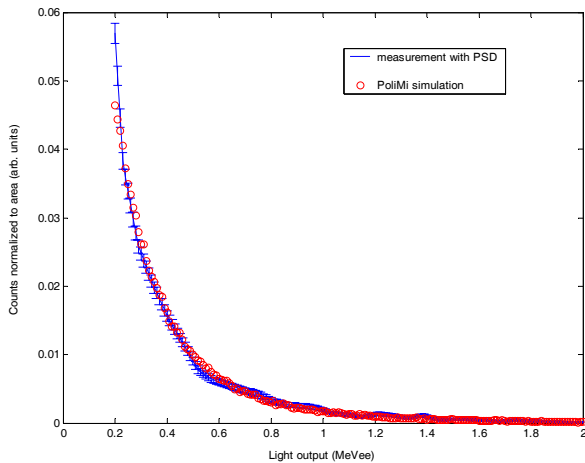


Fig. 12. Measurement versus simulation for the case Cf-252 – 1-in. Pb shield.

Figs. 13 and 14 show the neutron pulse-height distributions from the Am-Be with no shield and 1-in. Pb shield, respectively. As in the cases with the Cf-252 source, a very good agreement has been achieved, even though the Am-Be source was simulated as an isotropic source without any

additional construction material. In reality, the Am-Be source is surrounded with several inches of PE with an opening on one side. In addition, a stainless-steel layer with a varying thickness is a part of the source assembly. Fig. 9 shows a photograph of the source configuration.

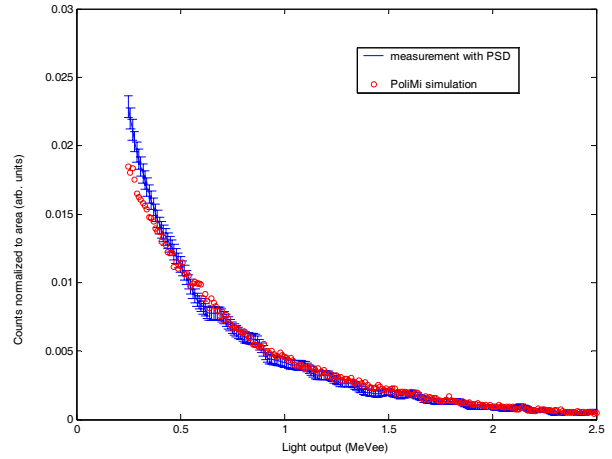


Fig. 13. Measurement versus simulation for the case Am-Be – no shield.

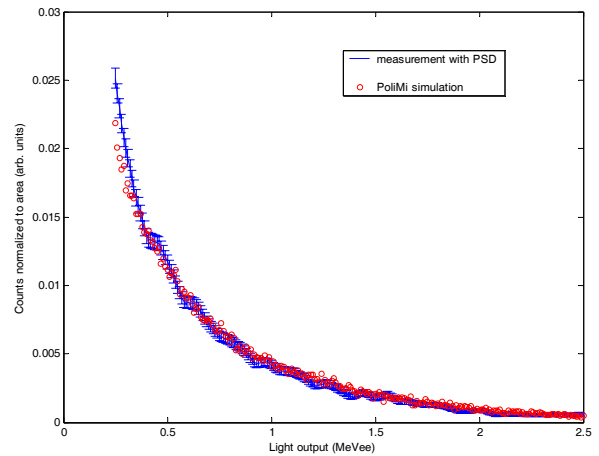


Fig. 14. Measurement versus simulation for the case Am-Be – 1-in. Pb shield.

Figs. 15 and 16 show the measured pulse-height distributions for the Cf-252 and Am-Be sources and for different experimental configurations. In both cases, no significant difference is observed in the pulse-height distributions with the shields used in the experiments. This is a very encouraging observation because it means that even with a certain shielding between the source and the detector measurements result in similar pulse-height distributions. In Fig. 17 we compare the pulse-height distributions shown in Figs. 15 and 16. Clearly, the Cf-252 and Am-Be sources can be easily distinguished from each other even without unfolding the initial neutron spectra. The logarithmic scale is used in Fig. 17.

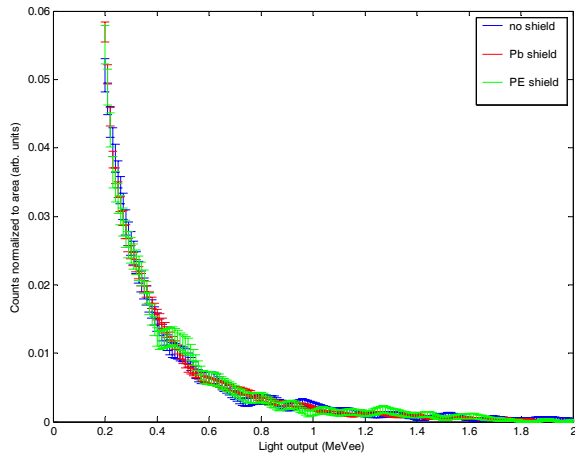


Fig. 15. Measured pulse-height distributions for the Cf-252 source in different experimental configurations.

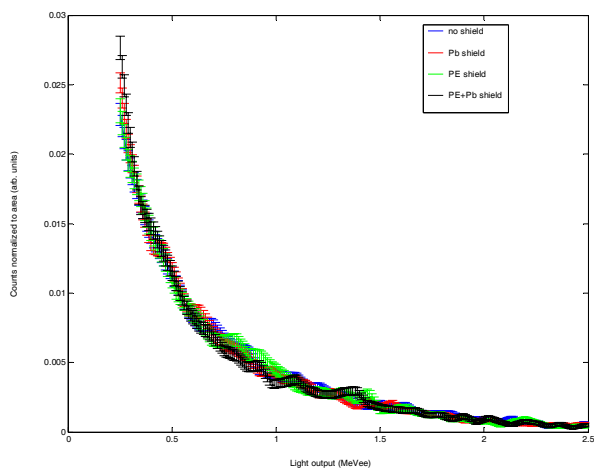


Fig. 16. Measured pulse-height distributions for the Am-Be source in different experimental configurations.

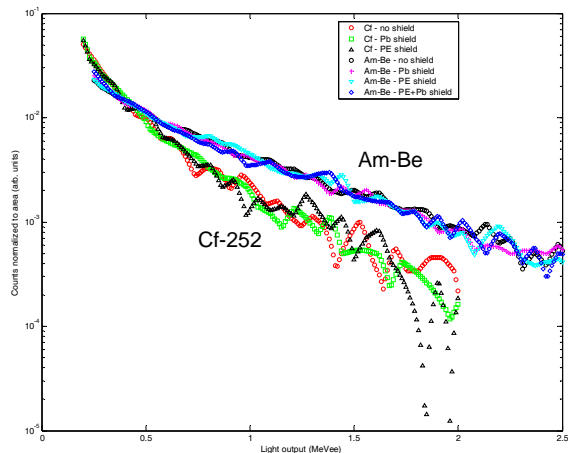


Fig. 17. Comparison between measured pulse-height distributions for the Cf-252 and Am-Be sources, shown in logarithmic scale. The error bars are not shown.

In Fig. 17 a large fluctuation of data is observed for high light output values, especially for the Cf-252 source with a 1-in. PE shield. This is caused by poor statistics, which is the consequence of the lack of the neutron pulses producing large enough light pulses.

VI. CONTINUING WORK

In the present work, several shields with various thicknesses are being tested with different neutron sources. This investigation will provide us with the practical limit of the source identification method presented in this paper.

There are several unfolding techniques available, which could be applied to pulse-height distributions obtained by neutron discrimination of measured data. Examples are sequential least-square method, neural networks, or inverse method [5]. These techniques are currently being tested to choose the most suitable unfolding method for this project. In addition, after the unfolding method has been chosen, an additional optimization of unfolding procedures will be necessary.

VII. CONCLUSIONS

An optimized digital fast pulse-shape discrimination algorithm was used to discriminate neutrons from gamma rays originating from unknown sources. The discriminated data was used to create pulse-height distributions for Cf-252 and Am-Be sources. These distributions were subsequently compared with simulations performed with the MCNP-PoliMi code. In all cases, very good agreement was achieved between simulations and measurements. In addition, several source-shielding configurations were tested to assess the influence of the potential source shielding on the neutron pulse-height distribution. It can be concluded that no significant changes can be expected for 1-in. shields made of Pb and PE, used separately or in combination. In all cases, the Am-Be source produces pulse-height distributions that are distinct when compared with those produced by the Cf-252 source. This makes the identification of the neutron sources with very different energy spectrum straightforward.

ACKNOWLEDGMENT

The authors thank Paul Hausladen from the Oak Ridge National Laboratory, Tennessee, for fruitful discussions on pulse-shape discrimination methods.

REFERENCES

- [1] G. F. Knoll, *Radiation Detection and Measurement*, 3rd ed., New York: Wiley, pp. 230, 565, 2000.
- [2] S. D. Jastaniah and P. J. Sellin, "Digital pulse-shape algorithms for scintillation-based neutron detectors," *IEEE Trans. Nucl. Sci.*, vol. 49, pp. 1824–1828, 2002.
- [3] Z. W. Bell, "Tests on a digital neutron-gamma pulse shape discriminator with NE213," *Nucl. Instr. Meth.*, vol. 188, pp. 105–109, 1981.
- [4] J. A. Mullens, J. D. Edwards, and S. A. Pozzi, "Analysis of Scintillator Pulse-Height for Nuclear Material Identification," *Institute of Nuclear Materials Management*, 45th Annual Meeting, Orlando, Florida, July 18–22, 2004.

- [5] Y. Xu, T. Downar, S. Avdic, V. Protopopescu, and S. A. Pozzi, "Techniques for Neutron Spectrum Unfolding from Pulse Height Distributions Measured with Liquid Scintillators," *Institute of Nuclear Materials Management*, Annual Meeting, Nashville, Tennessee, July 16–20, 2006.
- [6] S. A. Pozzi, E. Padovani, and M. Marseguerra, "MCNP-PoliMi: A Monte Carlo Code for Correlation Measurements," *Nucl. Instr. Meth. A*, vol. 513, pp. 550–558, 2003.
- [7] L. M. Bollinger and G. E. Thomas, "Measurement of the Time Dependence of Scintillation Intensity by a Delayed-Coincidence Method," *Rev. Sci. Instrum.*, vol. 32, p. 1044, 1961.
- [8] M. Moszynski et al., "Study of N-Gamma Discrimination with NE213 and BC501A Liquid Scintillators of Different Size," *Nucl. Instr. Meth. A*, vol. 350, pp. 226–234, 1994.
- [9] S. A. Pozzi, "Recent Developments in the MCNP-PoliMi Postprocessing Code," *Oak Ridge National Laboratory*, ORNL/TM-2004/299, 2004.